Published in final edited form as:
Biochemistry. 2008 December 30; 47(52): 13736–13744. doi:10.1021/bi8017625.

Formation and Function of the Manganese(IV)/Iron(III) Cofactor in *Chlamydia trachomatis* Ribonucleotide Reductase†

Wei Jiang[a,b,*], **Danny Yun**[a,c], **Lana Saleh**[a,d], **J. Martin Bollinger Jr.**[a,b,*], and **Carsten Krebs**[a,b,*]

a*Department of Biochemistry and Molecular Biology, The Pennsylvania State University, University Park, Pennsylvania 16802*

b*Department of Chemistry, The Pennsylvania State University, University Park, Pennsylvania 16802*

Abstract

The β_2 subunit of a class Ia or Ib ribonucleotide reductase (RNR) is activated when its carboxylate-bridged $Fe_2^{II/II}$ cluster reacts with O_2 to oxidize a nearby tyrosine (Y) residue to a stable radical (Y•). During turnover, the Y• in β_2 is thought to reversibly oxidize a cysteine (C) in the α_2 subunit to a thiyl radical (C•) by a long-distance (~35 Å) proton-coupled electron-transfer (PCET) step. The C• in α_2 then initiates reduction of the 2' position of the ribonucleoside-5'-diphosphate substrate by abstracting the hydrogen atom from C3'. The class I RNR from *Chlamydia trachomatis* (*Ct*) is the prototype of a newly recognized subclass (I*c*), which is characterized by the presence of a phenylalanine (F) residue at the site of β_2 where the essential radical-harboring Y is normally found. We recently demonstrated that *Ct* RNR employs a heterobinuclear Mn^{IV}/Fe^{III} cluster for radical initiation. In essence, the Mn^{IV} ion of the cluster functionally replaces the Y• of the conventional class I RNR. The *Ct* β_2 protein also auto-activates by reaction of its reduced (Mn^{II}/Fe^{II}) metal cluster with O_2. In this reaction, an unprecedented Mn^{IV}/Fe^{IV} intermediate accumulates almost stoichiometrically and decays by one-electron reduction of the Fe^{IV} site. This reduction is mediated by the near-surface residue, Y222, a residue with no functional counterpart in the well-studied conventional class I RNRs. In this review, we recount the discovery of the novel Mn/Fe redox cofactor in *Ct* RNR and summarize our current understanding of how it assembles and initiates nucleotide reduction.

Ribonucleotide reductases (RNRs) catalyze the reduction of ribonucleotides to deoxyribonucleotides, the building blocks for DNA. They provide the only *de novo* pathway for deoxyribonucleotide synthesis and are thus essential to all known life. Their central role in nucleotide metabolism makes them important targets for anticancer and antiviral therapeutics (1). It is thought that the evolution of the first RNR initiated the transition from the use of RNA as the primary information-encoding molecule (in the “RNA world”) to the use of DNA (in the “DNA world”) (2,3).

The RNR reaction involves replacement by hydrogen of the hydroxyl group on the 2'-carbon of the nucleoside di- or tri-phosphate (NDP or NTP) substrate. This chemically difficult

†This work was supported by the National Institutes of Health (GM-55365 to JMB and CK), the Beckman Foundation (Young Investigator Award to CK), and the Dreyfus Foundation (Teacher Scholar Award to CK).

Please send correspondence to: Wei Jiang, Department of Chemistry, 318 Chemistry Building, University Park, PA, Phone: 814-863-5685, Fax: 814-865-2927. J. Martin Bollinger, Jr., Department of Chemistry, 336 Chemistry Building, University Park, PA 16802, Phone: 814-863-5707, Fax: 814-865-2927. Carsten Krebs, Department of Chemistry, 332 Chemistry Building, University Park, PA 16802, Phone: 814-865-6089, Fax: 814-865-2927.
[c]Present address: Department of Biology, Massachusetts Institute of Technology, Cambridge, Massachusetts 02139
[d]Present address: New England Biolabs, 240 County Rd., Ipswich, Massachusetts 01938

replacement occurs by a free-radical mechanism (4). Evidence suggests that all known RNRs share a common fundamental strategy for catalysis, in which a transient cysteine thiyl radical (C•) in the active site (5–8) initiates the reduction by abstracting the 3'-hydrogen atom (9). Following replacement of the 2'-hydroxyl group by a hydrogen, the H• is returned to C3', regenerating the C•.

Although all RNRs apparently use this catalytic strategy, none possesses a C• in its resting state. Rather, the 3'-H-abstracting radical is produced at the beginning of each turnover and reduced back to the resting cysteine at the end (10–12). RNRs from different organisms have been divided into three classes primarily on the basis of the cofactor and mechanism that each employs for reversible C• production (2,4). The enzymes from aerobically growing *Escherichia coli* (*Ec*), most eukaryotes (including all mammals), and herpes simplex I virus belong to class I. The C•-generating cofactor in each of these RNRs is a stable tyrosyl radical (Y•) in close proximity to a (μ-oxo)-$Fe_2^{III/III}$ cluster (12,13). The cofactor is found in the enzyme's homodimeric β_2 subunit. It is generated when the $Fe_2^{II/II}$ form of the cluster reacts with O_2 to oxidize the Y residue by one electron to the Y• (13) (*vide infra*). The active holoenzyme is a dissociable 1:1 complex[2](14) of the homodimeric β_2 subunit and the homodimeric catalytic subunit, α_2, which contains the active site for substrate reduction and the binding sites for allosteric effectors (2). To initiate turnover, the Y• in β_2 oxidizes the cysteine residue in α_2 to the C• by a long-distance, inter-subunit, proton-coupled electron transfer (PCET) reaction (12) (*vide infra*).

Class I RNRs have been further sub-classified as a–c. The Ia (e.g., from mammals) and Ib (e.g., from *Salmonella typhimurium*) enzymes both use the $Fe^{III/III}$-Y• cofactor but differ from each other in primary structure, allosteric regulatory behavior, and preference for the protein source of electrons for nucleotide reduction (3). These differences are functionally less profound than their shared difference from the Ic RNR(s). This third and most recently recognized sub-class, of which the enzyme from the human pathogen, *Chlamydia trachomatis* (*Ct*), is the founding member, is defined by the replacement of the radical-harboring Y in the β_2 subunit with the redox incompetent F (15,16). We recently solved the seven-year mystery of how a class I RNR can be active without the initiating Y• by demonstrating that *Ct* RNR employs a stable, heterobinuclear, Mn^{IV}/Fe^{III} cofactor to initiate catalysis (17). Although the novel cofactor and radical-initiation strategy were just discovered, extensive analogy to the more well-characterized class Ia *Ec* enzyme has served to focus initial studies, so that considerable insight has rapidly emerged and detailed working hypotheses can already be advanced. For proper context, we must briefly summarize what is known about the formation and function of the *Ec* RNR $Fe_2^{III/III}$-Y• cofactor before reviewing these studies on the novel *Ct* enzyme.

Activation of Ec β_2

In assembly of the $Fe_2^{III/III}$-Y• cofactor, the $Fe_2^{II/II}$ cluster reacts with O_2 to oxidize the buried tyrosine residue (Y122) by one electron (18,19). The O_2-reactive complex forms spontaneously *in vitro* upon addition of Fe^{II} to apo β_2, but it is possible that accessory factors (e.g., an iron chaperone) are involved *in vivo*. The reduced protein can also form by *in situ* reduction of the $Fe_2^{III/III}$ cluster in the "met" protein (lacking the Y•). Indeed, reactivation of β_2 that has lost its Y• occurs by this mechanism *in vivo* and has been termed the "maintenance pathway" (20). The Fe_2S_2-containing ferredoxin, YfaE, and the flavodoxin, NrdI, have been identified as proteins that effect the $Fe_2^{III/III} \rightarrow Fe_2^{II/II}$ conversion for the class Ia and Ib β_2s, respectively (21–23).

[2]Some class I RNRs, e.g., the enzyme from *Homo sapiens*, can also have $\alpha_4\beta_4$ and $\alpha_6\beta_6$ composition under certain conditions (14).

The mechanism of activation of wild-type (wt) *Ec* β_2 was investigated by a combination of rapid kinetic and spectroscopic methods (Figure 1, top) (12). An intermediate, termed **X**, was shown to be kinetically competent to oxidize Y122 in the last, slowest step of the reaction carried out in the presence of reductant [e.g., ascorbate] (19,24). **X** has an $S = 1/2$ ground state that gives rise to a sharp, nearly isotropic $g = 2.0$ signal in the X-band EPR spectrum. Mössbauer and ^{57}Fe-ENDOR spectroscopies revealed that the $S = 1/2$ ground state is a consequence of antiferromagnetic coupling between high-spin Fe^{III} ($S = 5/2$) and Fe^{IV} ($S = 2$) sites (25). **X** has been subjected to extensive spectroscopic (X-ray absorption, ^{1}H-, ^{2}H-, and ^{17}O-ENDOR, and MCD) and computational analysis (26–29).

The complete reduction of O_2 at the Fe_2 cluster requires four electrons, of which three are provided by the oxidation of the reduced $Fe_2^{II/II}$ cofactor to generate the $Fe_2^{III/IV}$ intermediate, **X**. The transfer of the forth ("extra") electron to the diiron site is mediated by the near-surface residue, W48, which is transiently oxidized to a tryptophan cation radical (W48+•) (30,31). *In vitro*, the W48+• is subsequently reduced by an exogenous reductant (e.g., ascorbate, a thiol, or Fe^{II}_{aq}) (31). The *in vivo* reductant for the W48+• remains unclear, but the ferrodoxin YfaE is a candidate (21).

Intermediates occurring before the **X**-W48+• state barely accumulate during activation of wt *Ec* β_2 (31,32) but have been observed in variants of the *Ec* protein and in the wt β_2 from mouse [*Mus musculus* (*Mm*)]. A (μ-1,2-peroxo)-$Fe_2^{III/III}$ intermediate, which exhibits spectroscopic properties similar to those of the (μ-1,2-peroxo)-$Fe_2^{III/III}$ intermediate, $\mathbf{H}_{peroxo}$ (or **P**), in the reaction of soluble methane monooxygenase (33), was observed in *Ec* β_2 variants with the ligand substitution D84E (34,35) and, more importantly, in wt *Mm* β_2 (36). Insight into the immediate precursor to the **X**-W48+• state was provided by studies on the *Ec* β_2 W48A/Y122F variant. 3-Methylindole was used as an analogue of the truncated W48 sidechain to chemically trigger the ET step needed to form **X** (37). This precursor state comprises at least two distinct antiferromagnetically coupled $Fe_2^{III/III}$ clusters, which may be protonated successors to the (μ-1,2-peroxo)-$Fe_2^{III/III}$ intermediate.

PCET between α_2 and β_2

The distance in the *Ec* RNR holoenzyme between the Y• in β_2 and the C•-forming cysteine (C439) in α_2 is unknown but is ~ 35 Å in a "docking" model generated from the structures of the individual subunits (8). This model has been validated by pulsed electron-electron double resonance (PELDOR) and double quantum coherence (DQC) measurements (38,39). The rate constant for ET by a single electron-tunneling step over this long distance would be 10^{-4} – 10^{-9} s^{-1}, which is far too slow to account for the single-turnover and steady-state rate constant of ~ 10 s^{-1} (25 °C) for *Ec* RNR (12). Rather, the ET is mediated by a chain of conserved, hydrogen-bonded, aromatic amino acids, including W48 and Y356 in *Ec* β_2 and Y731 and Y730 in *Ec* α_2 (Figure 2C), which form transient radicals in an "electron relay" mechanism (12). These residues are conserved in all known class I RNRs, and substitution of any of them by F leads to drastic diminution of activity (40–43). Further, the ET step is believed to be coupled to proton transfer (proton-coupled electron transfer or PCET). In the absence of environmental effects, pure ET (not proton-coupled) from a neutral C to a neutral Y• to give a Y–/C+• state should be unfavorable. However, PCET to give a state with neutral constituents (Y/C•) is expected to be thermodynamically feasible (12). Thus, it is thought that the cysteine loses its proton and the tyrosine obtains a proton in the PCET step.

Two obstacles long thwarted the direct interrogation of the PCET step. First, the forward PCET to generate the C• is preceded by a slow physical step, which is gated by the binding of a substrate and allosteric effector (PCET is thus said to be "conformationally gated") (10). Consequently, intermediates are "kinetically masked." Second, although it is possible that the

proposed pathway radical intermediates might still accumulate to low levels, their spectroscopic properties (in particular EPR) are expected to be similar to those of Y122•, potentially preventing their detection. For these reasons, the studies of *Ec* β_2 activation stood for some time as the best evidence for a radical-hopping mechanism for ET to the cofactor. In addition to establishing the role of W48 in relaying the "extra" electron, they also showed that W48+• can (under the proper conditions) oxidize Y122 (30,31), which would be analogous to the last step in the reverse inter-subunit PCET from Y122 to the C•, and that a rapid redox equilibrium between W48 and Y356 is engaged in the presence of Mg^{2+} at concentrations similar to the 15 mM employed in the RNR activity assay (44).

Stubbe and co-workers have at last provided definitive evidence for the proposed electron-relay PCET mechanism. First, by replacing the subunit-interfacial pathway tyrosine in the β_2 subunit of the *Ec* enzyme (Y356) with mono- and poly-fluorinated tyrosines, they systematically varied the radical-reduction potential and pK_a of this pathway position. The catalytic activities (and their dependence on pH) of these variants established both the narrow range of reduction potential required for functional PCET and that the Y356 phenolic proton is not obligatorily transferred (45). Second, by replacing any of the three pathway tyrosines (Y356 in β_2; Y730 and Y731 in α_2) with a more easily oxidized analogue, they engineered depressions in the free-energy profile for the radical-hopping process, causing the radical to reside on the unnatural residue upon engagement of the ready holoenzyme complex (45–48). Importantly, the Y730/Y731→3-aminotyrosine (NH_2Y) α_2s retain significant catalytic activity, and the NH_2Y radicals detected in these variants are kinetically competent to be on the catalytic pathway (48).

Discovery of the Y•-less class I (Ic) RNR(s)

McClarty and co-workers isolated and sequenced the genes encoding the subunits of a class I RNR from the pathogenic intracellular parasite, *Chlamydia trachomatis* (*Ct*) (15). Comparison of the predicted protein sequences to those of other RNR subunits revealed conservation of all but one of the β_2 cofactor ligands and all but one of the α_2 and β_2 PCET pathways residues (Figure 2). The important exceptions are the replacements of the radical-harboring Y by a redox-inert phenylalanine (F127) and the Fe1 aspartate ligand (D84 in *Ec* β_2) by glutamate (E89 in *Ct* β_2). The crystal structure of *Ct* β_2 confirmed that F127 is located at the site where the radical harboring tyrosine is normally found (16). Despite the absence of the radical-harboring Y, the *Ct* RNR produced in and isolated from *Ec* was found to be catalytically active, suggesting a fundamentally different strategy to generate the C• in the α_2 subunit (15). The Y→F and D→E non-identities are also found in (hypothetical) β_2 proteins from other organisms, including the human pathogens *Mycobacterium tuberculosis* and *Tropheryma whipplei* (16). A third sub-class, Ic, was founded to comprise these Y•-less RNRs.

Nordlund, Gräslund, McClarty and co-workers proposed that the $Fe_2^{III/IV}$ cluster, **X**, which they detected in the *Ct* β_2 protein by EPR spectroscopy, functionally replaces the Y• of the conventional class I RNRs (16,49). In support of this hypothesis, the stability of **X** was shown to be enhanced by the presence of α_2 (49). We recently confirmed an essential aspect of this innovative hypothesis: *Ct* RNR does indeed use a high-valent metal ion in place of the conventional Y• as radical initiator. However, the $Fe_2^{III/IV}$ complex of β_2 is not its active form. Rather, *Ct* RNR employs a Mn^{IV}/Fe^{III} cofactor (50) to initiate catalysis (17).

Discovery of the Mn-requirement of class Ic RNRs

We began our study of *Ct* RNR by measuring the catalytic activities of preparations of β_2 that had been isolated from different media and subjected to different metal-chelation and reconstitution procedures (17). We expected on the basis of the published hypothesis and previous studies on the *Ec* enzyme (51) to find a tight correlation between activity and iron

content (Figure 3A). *Ct* β_2 emerged from the over-producing *Ec* cells grown in rich medium with 0.75 Fe/β and a turnover number of 0.035 s^{-1}/β, which is less than the value reported by the Gräslund group [0.05 s^{-1} (49)] and < 1% the optimal activity of the *Ec* protein (12). Addition of Fe^{II} in the presence of O_2 to reconstitute these preparations to full cofactor content (theoretically 2 Fe/β) failed to increase activity. A reductive chelation procedure removed almost all the iron (leaving < 0.05/β) and – as expected – diminished activity (to ≤ 0.008 s^{-1}), but subsequent reconstitution of these preparations with excess Fe^{II} and O_2 increased activity only marginally, if at all (to ≤ 0.010 s^{-1}). *Ct* β_2 purified from cells grown in the presence of the Fe^{II}-chelator, 1,10-phenanthroline, had very little iron (< 0.05), but greater than expected activity (0.025 s^{-1}). Addition of excess Fe^{II} to this protein in the presence of excess O_2 increased its activity only slightly (to ≤ 0.035 s^{-1}). Finally, preparations from cells grown on minimal medium supplemented with iron had the same Fe content (~ 0.75 Fe/β) as protein from rich medium but less than one-tenth its activity (~ 0.003 s^{-1}). The absence of the expected correlation between iron content and enzyme activity suggested the possibility of an additional cofactor component (17).

In parallel, we examined the *Ct* β_2 preparations subjected to the above and other treatments by a combination of spectroscopic methods. A multi-line, $g \sim 2$ EPR spectrum (Figure 3B) exhibited by preparations reconstituted with Fe^{II} and then briefly treated with an excess of the strong reductant, dithionite (17), was the crucial clue. Use of $^{57}Fe^{II}$ (with nuclear spin quantum number, I, of 1/2) in this treatment led to the broadening of several lines, indicating that the associated complex contains Fe. The multiple lines suggested hyperfine coupling to an additional transition metal with a high value of I, e.g., ^{55}Mn with $I = 5/2$. Aware of an earlier report of a similar EPR spectrum from a Mn^{III}/Fe^{III} complex (52), we considered that the dithionite-reduced *Ct* β_2 might harbor such a cluster. Following this spectroscopic clue, we examined the dependence of catalytic acitivity on the Mn/Fe ratio. Two equiv of total metal ions was added to the metal-depleted protein with varying mole-fractions of Mn and Fe, and the activity was monitored in the presence of O_2 (Figure 3C) (17). Addition of either Fe^{II} or Mn^{II} alone resulted in *no significant increase* over the residual activity (0.005–0.008 s^{-1}/β) of the metal-depleted protein (a key point discussed further below), whereas addition of one equiv of each M^{II} activated by a factor of more than 50 (17). These results strongly suggested that *Ct* β_2 uses a Mn/Fe cofactor rather than a Fe_2 cofactor.

A Mn^{IV}/Fe^{III} product from reaction of the Mn^{II}/Fe^{II}-β_2 complex with O_2

Reasoning by analogy to the conventional class I RNRs that the function of the *Ct* β_2 cofactor should be to oxidize the conserved cysteine in *Ct*α_2 (C672) to the C•, we anticipated that the reduced Mn^{II}/Fe^{II}-β_2 complex would be inactive and would be activated by reaction with O_2. We verified this expectation by showing that addition of the O_2-free Mn^{II}/Fe^{II}-β_2 complex to an RNR reaction solution also lacking O_2 did not result in turnover, whereas prior exposure of the complex to O_2 gave maximal activity, irrespective of the presence of O_2 in the subsequent RNR reaction (17). The stable (half-life of at least hours at 5 °C) product of the O_2 reaction is, by contrast to the active, Y•-containing forms of the conventional β_2 proteins, EPR-silent.[3] It exhibits a quadrupole doublet in the 4.2-K/zero-field Mössbauer spectrum (Figure 1). The isomer shift, δ= 0.52 mm/s, indicates the presence of a high-spin Fe^{III} site. Its Mössbauer spectra in varying magnetic field show that it has a $S_{Total} = 1$ ground state, which could most simply arise from antiferromagnetic coupling of the $S_{Fe} = 5/2$ Fe^{III} ion with an $S_{Mn} = 3/2$ Mn^{IV} site (50). The demonstration that the aforementioned dithionite treatment giving the ^{55}Mn- and ^{57}Fe-coupled $g \sim 2$ EPR signal *does not change the oxidation state of the* Fe^{III} *site* confirmed this assignment by establishing that the $S_{Total} = 1/2$ ground state of the

[3]The absence of an EPR signal from the active form was at least partly responsible for the ~ 7-year interval between the discovery of the Y•-less *Ct* β_2 and the correct identification of its functional cofactor.

dithionite-treated form arises from antiferromagnetic coupling of S_{Fe} = 5/2 Fe^{III} and S_{Mn} = 2 Mn^{III} ions (17). Thus, the product of the O_2 reaction in *Ct* β_2 (before its reduction by dithonite) is a Mn^{IV}/Fe^{III} complex. Like the product of the cognate reaction in a conventional β_2, it is more oxidized than the $M_2^{II/II}$ reactant by three electrons (Figure 1).

The Mn^{IV} site functionally replaces the Y• of a conventional class I RNR

The next question was whether this stable product is the active form of *Ct* β_2. The inactivity of the dithionite-reduced Mn^{III}/Fe^{III} form was consistent with this possibility. The substrate analog, 2'-azido-2'-deoxyadenosine-5'-diphosphate (N_3-ADP), was used to confirm that the Mn^{IV}/Fe^{III} complex is the active form (17). In previous studies on *Ec* RNR, it had been shown that treatment with the 2'-azido-substituted nucleotide causes irreversible reduction of the Y• (53) along with formation of a meta-stable, nitrogen-centered radical (N•) (54) in which a cysteine of the enzyme is covalently linked to C3' via its sulfur and an N_3-derived nitrogen (55). Our expectation was that N_3-ADP would cause irreversible one-electron reduction of the *Ct* RNR radical initiator, resulting in conversion of the EPR-silent Mn^{IV}/Fe^{III} state to the EPR-active Mn^{III}/Fe^{III} state, together with formation of the N•. The spectrum of the N• was indeed observed. In addition, a spectrum with hyperfine coupling to both ^{55}Mn and ^{57}Fe was seen to develop in the N_3-ADP reaction but not in the reaction with the normal substrate, CDP. Although much sharper and more featured than the spectrum produced by dithionite treatment of β_2 in isolation, this spectrum was also seen upon dithionite treatment of the holoenzyme under turnover conditions.[4](56) Parameters (**g**, $\mathbf{A}_{Mn}$, and $\mathbf{A}_{Fe}$) extracted by simulation of the spectrum, as well as more recent (unpublished) variable-field Mössbauer spectroscopic characterization of the N_3-ADP-generated species, establish that its cluster is in the Mn^{III}/Fe^{III} oxidation state. The reduction of the cluster by one-electron concomitantly with accumulation of the N• establish that the EPR-silent, Mn^{IV}/Fe^{III} cluster is the radical initiator in *Ct* RNR. The observations also indicate that the EPR spectrum, and thus the structure, of the Mn^{III}/Fe^{III} cluster are sensitive to whether it is generated in isolated β_2 or the functioning holoenzyme. Presumably, binding of β_2 to α_2(•CDP•ATP) causes a conformational change that is communicated to the cluster site. This change is likely to reflect the conformational gate for the PCET step (57).

After we had reported the activity of the Mn^{IV}/Fe^{III} form of *Ct* β_2, the Gräslund group published a study also recognizing this fact (56). However, they interpreted their data to indicate that the $Fe_2^{III/IV}$ form is also active (albeit less so). Our data are inconsistent with this view (17). Addition of Fe^{II} alone (in the presence of O_2) to metal-depleted (< 0.05 Fe/β) β_2 results in *no significant increase in its RNR activity* (< 50 % increase), even though the protein takes up the added Fe^{II} and accumulates the $Fe_2^{III/IV}$ state, **X**. By contrast, the optimized (Mn^{II} + Fe^{II}) reconstitution procedure activates by ~ 100-fold (10,000 %). Moreover, treatment of the holoenzyme containing **X** in β_2 with N_3-ADP does not accelerate the very slow decay of **X** nor cause accumulation of the N•. We view these observations as compelling evidence that the $Fe_2^{III/IV}$ β_2 is inactive (17) (but confess to being surprised by this fact).

A Mn^{IV}/Fe^{IV} intermediate during activation of Ct β_2

Further analysis of the activation reaction revealed accumulation of a novel Mn^{IV}/Fe^{IV} intermediate followed by the one-electron reduction of the Fe^{IV} site to give the active form (58). The Mn^{IV}/Fe^{IV} intermediate exhibits a broad optical feature centered near 390 nm and a sharp *g* ~ 2 EPR signal with six lines (from hyperfine coupling to a single ^{55}Mn nucleus) separated by ~ 80 G. When the intermediate contains ^{57}Fe, the sextet signal also shows

[4]After we reported the spectrum of the Mn^{III}/Fe^{III} cluster generated by treatment of the holoenzyme with either dithionite or N_3-ADP, Gräslund and co-workers reported that treatment with hydroxyurea can generate the same spectrum (56).

hyperfine coupling to this $I = 1/2$ nucleus (Figure 1). The $\mathbf{A}_{Mn}$ tensor extracted from EPR simulation analysis is nearly isotropic (247, 216, 243 MHz), similar to A_{Mn} for the Mn^{IV} site in catalase (59). The Mössbauer isomer shift of the iron site ($\delta = 0.17 \pm 0.06$ mm/s) is indicative of the +IV oxidation state and is similar to that observed for the $Fe_2^{IV/IV}$ complex, **Q**, in the reaction of sMMOH (33,60). Field-dependent Mössbauer spectra show that the Fe^{IV} site is in the high spin ($S_{Fe} = 2$) configuration. Antiferromagnetic coupling between the Fe^{IV} ($S_{Fe} = 2$) and the Mn^{IV} ($S_{Mn} = 3/2$) ions results in the $S = 1/2$ ground state (58). To our knowledge, the Mn^{IV}/Fe^{IV} complex has no precedent in either inorganic chemistry or biochemistry. It is the cognate of the $Fe_2^{IV/IV}$ intermediate **Q** from sMMO (33,60,61). It is likely to have a *bis*-μ-oxo-Mn^{IV}/Fe^{IV} "diamond core" structure, as was suggested for **Q** (62). The crystal structure of the $Fe_2^{III/III}$ form of β_2 revealed the presence of two solvent (water or hydroxo) bridges (16) (Figure 2A), which contrasts with the single oxo-bridge found in the class Ia (63) (Figure 2B) and Ib β_2s (64). This difference suggests that the *Ct* β_2 site could be adapted to stabilize the diamond core in the Mn^{IV}/Fe^{IV} and Mn^{IV}/Fe^{III} states. Formation of the Mn^{IV}/Fe^{IV} intermediate is first order in $[O_2]$ ($k_{form} = 13 \pm 3$ $mM^{-1}s^{-1}$ at 5 °C) (58). Thus, intermediates preceding the Mn^{IV}/Fe^{IV} state [e.g., a peroxo-Mn^{III}/Fe^{III} analogue of the μ-1,2-peroxo-$Fe_2^{III/III}$ complex detected during activation of the *Mm* (36) and *Ec* (32) proteins] do not accumulate. The EPR-active, $S = 1/2$ ground state of the Mn^{IV}/Fe^{IV} intermediate makes it amenable to structural characterization by multinuclear paramagnetic resonance methods (27), an opportunity not afforded by the homobinuclear homolog, **Q**, with its diamagnetic ground state.

Evidence for branched electron-relay pathways in Ct β_2

The Mn^{IV}/Fe^{IV} state decays to the stable Mn^{IV}/Fe^{III} state by transfer of the "extra" electron to the Fe^{IV} site (58). The "intrinsic" decay rate constant is 0.02 ± 0.005 s^{-1} (5 °C), and the process is accelerated by the reductant, ascorbate, with a second order rate constant of 1.3 ± 0.3 $mM^{-1}s^{-1}$ (58). In activation of *Ec* β_2, the "extra" electron is relayed to the cluster by W48, which is transiently oxidized to the W48+• (31). In *Ct* β_2, the surface residue Y222 plays a key role in the electron relay (65). The rate constants for intrinsic decay and ascorbate reduction are diminished by 10-fold and 65-fold (respectively) in the Y222F variant. The same product (the Mn^{IV}/Fe^{III} cluster) still forms, and the Y222F protein is then as active as the wt protein, establishing that Y222 is not part of the inter-subunit PCET pathway (Figure 2D). Conversely, substitution of Y338, the counterpart of the subunit-interfacial PCET-pathway residue (Y356) in *Ec* β_2 (47), with F does not affect the kinetics of the activation reaction but diminishes catalytic activity to an undetectable level. Substitution of W51, the counterpart of *Ec* β_2 W48, with F compromises both activation and catalysis, marking this residue as the branch point for the activation- and catalysis-specific pathways (65).

Reaction of the Mn^{II}/Fe^{II} and Mn^{II}/Fe^{II} forms with H_2O_2

Before our identification of its unique cofactor, it had been suggested that the Y•-less class Ic β_2s might have evolved to tolerate oxidative stress imposed by the host's immune response (16). Our examination of the reactivities of the Mn^{IV}/Fe^{III}, Mn^{III}/Fe^{III}, and Mn^{II}/Fe^{II} forms of *Ct* β_2 toward hydrogen peroxide, an important host-generated reactive oxygen species (ROS), is consistent with this notion (66). Activity of the Mn^{IV}/Fe^{III} form is completely stable in the presence of H_2O_2. The inactive, one-electron-reduced Mn^{III}/Fe^{III} form is rapidly (8 ± 1 $M^{-1}s^{-1}$ at 5 °C) and quantitatively (> 90%) reactivated by H_2O_2 via the Mn^{IV}/Fe^{IV} intermediate. The fully-reduced Mn^{II}/Fe^{II} form is also efficiently activated in a three-step reaction through Mn^{III}/Fe^{III} and Mn^{IV}/Fe^{IV} intermediates (see Figure 1). The propensity of *Ct* β_2 to become fully active upon exposure to H_2O_2 essentially irrespective of its initial redox state represents a potentially relevant contrast to the behavior of the *Ec* protein. Although its fully-reduced ($Fe_2^{II/II}$) state reacts readily with H_2O_2 to generate the "met" (Y•-less)

$Fe_2^{III/III}$ form, this form further reacts only very inefficiently to generate the active Y•-containing protein (67).

Outlook

Our recent work has demonstrated that Nature chose a decidedly bioinorganic solution to replacement of the radical-initiating Y•-$Fe_2^{III/III}$ cofactor of a conventional class I RNR: the use of a high-valent Mn^{IV} site in a Mn^{IV}/Fe^{III} cluster. To our knowledge, *Ct* RNR provides the first example of a heterobinuclear Mn/Fe redox cofactor in biology and the only uncontradicted evidence for a Mn-containing RNR.[5] (68,69) Its use of the Mn/Fe cofactor affords unique opportunities to dissect the conformationally-gated, inter-subunit, long-distance PCET. The absence of an EPR signal from the resting *Ct* enzyme could permit detection of even trace levels of pathway radicals that in the conventional RNRs might be obscured by the spectrum of the initiating Y•. In addition, by contrast to the best-studied conventional class I RNR from *Ec*, the reduced form of the cofactor (Mn^{III}/Fe^{III}) in *Ct* RNR is EPR-active, and its structure is apparently sensitive to remote binding events. Efforts to capitalize on these opportunities are underway.

Abbreviations

ATP, adenosine-5'-triphosphate
C•, cysteinyl radical
CDP, cytidine-5'-diphosphate
Ct, *Chlamydia trachomatis*
dCDP, 2'-deoxycytidine-5'-diphosphate
Ec, *Escherichia coli*
EPR, electron paramagnetic resonance
NH_2Y, 3-aminotyrosine
N_3-ADP, 2'-azido-2'-deoxyadenosine-5'-diphosphate
NDP, nucleoside-5'-diphosphate
dNDP, 2'-deoxynucleoside-5'-diphosphate
NTP, nucleoside-5'-triphosphate
PCET, proton-coupled electron transfer
RNR, ribonucleotide reductase
Y•, tyrosyl radical

Acknowledgment

We thank our colleagues whose work is reviewed herein.

REFERENCES

1. Licht, S.; Stubbe, J. Mechanistic investigations of ribonucleotide reductases. In: Poulter, CD., editor. Comprehensive natural products chemistry. New York: Elsevier; 1999. p. 163-203.
2. Nordlund P, Reichard P. Ribonucleotide reductases. Annu. Rev. Biochem 2006;75:681–706. [PubMed: 16756507]
3. Reichard P. The evolution of ribonucleotide reduction. Trends Biochem Sci 1997;22:81–85. [PubMed: 9066257]

[5]It was initially reported that the class I RNR from *Corynebacterium ammoniagenes* (formerly called *Brevibacterium ammoniagenes*) uses a Mn-containing cofactor of unknown composition (68). Recent studies suggest that this RNR can utilize the conventional Y•-$Fe_2^{III/III}$ cofactor (69). This controversy is one of several, recent, stark illustrations of the importance of *correlating catalytic activity* with metal (cluster) content of a redox metalloenzyme in identifying its functional cofactor.

4. Stubbe J, van der Donk WA. Protein radicals in enzyme catalysis. Chem. Rev 1998;98:705–762. [PubMed: 11848913]
5. Mao SS, Yu GX, Chalfoun D, Stubbe J. Characterization of C439SR1, a mutant of *Escherichia coli* ribonucleotide diphosphate reductase: evidence that C439 is a residue essential for nucleotide reduction and C439SR1 is a protein possessing novel thioredoxin-like activity. Biochemistry 1992;31:9752–9759. [PubMed: 1390751]
6. Mao SS, Holler TP, Yu GX, Bollinger JM Jr, Booker S, Johnston MI, Stubbe J. A model for the role of multiple cysteine residues involved in ribonucleotide reduction: amazing and still confusing. Biochemistry 1992;31:9733–9743. [PubMed: 1382592]
7. Licht S, Gerfen GJ, Stubbe J. Thiyl radicals in ribonucleotide reductases. Science 1996;271:477–481. [PubMed: 8560260]
8. Uhlin U, Eklund H. Structure of ribonucleotide reductase protein R1. Nature 1994;370:533–539. [PubMed: 8052308]
9. Stubbe J, Ackles D. On the mechanism of ribonucleoside diphosphate reductase from *Escherichia coli*. J. Biol. Chem 1980;255:8027–8030. [PubMed: 6997288]
10. Ge J, Yu G, Ator MA, Stubbe J. Pre-steady-state and steady-state kinetic analysis of *E.coli* class I ribonucleotide reductase. Biochemistry 2003;42:10017–10083.
11. Licht SS, Lawrence CC, Stubbe J. Class II ribonucleotide reductases catalyze carbon-cobalt bond reformation on every turnover. J. Am. Chem. Soc 1999;121:7463–7468.
12. Stubbe J, Nocera DG, Yee CS, Chang MCY. Radical initiation in the class I ribonucleotide reductase: long-range proton-coupled electron transfer? Chem. Rev 2003;103:2167–2202. [PubMed: 12797828]
13. Stubbe J. Di-iron-tyrosyl radical ribonucleotide reductases. Curr. Opin. Chem. Biol 2003;7:183–188. [PubMed: 12714050]
14. Kashlan OB, Scott CP, Lear JD, Cooperman BS. A comprehensive model for the allosteric regulation of mammalian ribonucleotide reductase. Functional consequences of ATP- and dATP-induced oligomerization of the large subunit. Biochemistry 2002;41:462–474. [PubMed: 11781084]
15. Roshick C, Iliffe-Lee ER, McClarty G. Cloning and characterization of ribonucleotide reductase from *Chlamydia trachomatis*. J. Biol. Chem 2000;275:38111–38119. [PubMed: 10984489]
16. Högbom M, Stenmark P, Voevodskaya N, McClarty G, Gräslund A, Nordlund P. The radical site in Chlamydial ribonucleotide reductase defines a new R2 subclass. Science 2004;305:245–248. [PubMed: 15247479]
17. Jiang W, Yun D, Saleh L, Barr EW, Xing G, Hoffart LM, Maslak M-A, Krebs C, Bollinger JM Jr. A manganese(IV)/iron(III) cofactor in *Chlamydia trachomatis* ribonucleotide reductase. Science 2007;316:1188–1191. [PubMed: 17525338]
18. Petersson L, Gräslund A, Ehrenberg A, Sjöberg B-M, Reichard P. The iron center in ribonucleotide reductase from *Escherichia coli*. J. Biol. Chem 1980;255:6706–6712. [PubMed: 6248531]
19. Bollinger JM Jr, Edmondson DE, Huynh BH, Filley J, Norton JR, Stubbe J. Mechanism of assembly of the tyrosyl radical-dinuclear iron cluster cofactor of ribonucleotide reductase. Science 1991;253:292–298. [PubMed: 1650033]
20. Hristova D, Wu C-H, Jiang W, Krebs C, Stubbe J. Importance of the maintenance pathway in the regulation of the activity of *Escherichia coli* ribonucleotide reductase. Biochemistry 2008;47:3989–3999. [PubMed: 18314964]
21. Wu C-H, Jiang W, Krebs C, Stubbe J. YfaE, a ferredoxin involved in diferric-tyrosyl radical maintenance in *Escherichia coli* ribonucleotide reductase. Biochemistry 2007;46:11577–11588. [PubMed: 17880186]
22. Roca I, Torrents E, Sahlin M, Gibert I, Sjöberg B-M. NrdI essentiality for class Ib ribonucleotide reduction in *Streptococcus pyogenes*. J. Bact 2008;190:4849–4858. [PubMed: 18502861]
23. Cotruvo JA Jr, Stubbe J. NrdI, an unusual flavodoxin involved in maintenance of the diferric-tyrosyl radical cofactor in *Escherichia coli* class Ib ribonucleotide reductase. Proc. Natl. Acad. Sci. U.S.A 2008;105:14383–14388. [PubMed: 18799738]
24. Bollinger JM Jr, Tong WH, Ravi N, Huynh BH, Edmondson DE, Stubbe J. Mechanism of assembly of the tyrosyl radical-diiron(III) cofactor of *E.coli* ribonucleotide reductase. 2. Kinetics of the excess

Fe^{2+} reaction by optical, EPR, and Mössbauer spectroscopies. J. Am. Chem. Soc 1994;116:8015–8023.

25. Sturgeon BE, Burdi D, Chen S, Huynh BH, Edmondson DE, Stubbe J, Hoffman BM. Reconsideration of **X**, the diiron intermediate formed during cofactor assembly in *E. coli* ribonucleotide reductase. J. Am. Chem. Soc 1996;118:7551–7557.
26. Riggs-Gelasco PJ, Shu L, Chen S, Burdi D, Huynh BH, Que L Jr, Stubbe J. EXAFS characterization of the intermediate **X** generated during the assembly of the *Escherichia coli* ribonucleotide reductase R2 diferric tyrosyl radical cofactor. J. Am. Chem. Soc 1998;120:849–860.
27. Burdi D, Willems J-P, Riggs-Gelasco P, Antholine WE, Stubbe J, Hoffman BM. The core structure of **X** generated in the assembly of the diiron cluster of ribonucleotide reductase: $^{17}O_2$ and $H_2{}^{17}O$ ENDOR. J. Am. Chem. Soc 1998;120:12910–12919.
28. Mitić N, Clay MD, Saleh L, Bollinger JM Jr, Solomon EI. Spectroscopic and electronic structure studies of intermediate **X** in ribonucleotide reductase R2 and two variants: a description of the Fe^{IV}-oxo bond in the Fe^{III}-O-Fe^{IV} dimer. J. Am. Chem. Soc 2007;129:9049–9065. [PubMed: 17602477]
29. Han W-G, Liu T, Lovell T, Noodleman L. Density functional theory study of Fe(IV) d-d optical transitions in active-site models of class I ribonucleotide reductase intermediate **X** with vertical self-consistent reaction field methods. Inorg. Chem 2006;45:8533–8542. [PubMed: 17029364]
30. Bollinger JM Jr, Tong WH, Ravi N, Huynh BH, Edmondson DE, Stubbe J. Mechanism of assembly of the tyrosyl radical-diiron(III) cofactor of *E.coli* ribonucleotide reductase. 3. Kinetics of the limiting Fe^{2+} reaction by optical, EPR, and Mösbauer spectroscopies. J. Am. Chem. Soc 1994;116:8024–8032.
31. Baldwin J, Krebs C, Ley BA, Edmondson DE, Huynh BH, Bollinger JM Jr. Mechanism of rapid electron transfer during oxygen activation in the R2 subunit of *Escherichia coli* ribonucleotide reductase. 1. Evidence for a transient tryptophan radical. J. Am. Chem. Soc 2000;122:12195–12206.
32. Tong WH, Chen S, Lloyd SG, Edmondson DE, Huynh BH, Stubbe J. Mechanism of assembly of the diferric cluster-tyrosyl radical cofactor of *Escherichia coli* ribonucleotide reductase from the diferrous form of the R2 subunit. J. Am. Chem. Soc 1996;118:2107–2108.
33. Liu KE, Valentine AM, Wang D, Huynh BH, Edmondson DE, Salifoglou A, Lippard SJ. Kinetic and spectroscopic characterization of intermediates and component interactions in reactions of methane monooxygenase from *Methylococcus capsulatus* (Bath). J. Am. Chem. Soc 1995;117:10174–10185.
34. Bollinger JM Jr, Krebs C, Vicol A, Chen S, Ley BA, Edmondson DE, Huynh BH. Engineering the diiron site of *Escherichia coli* ribonucleotide reductase protein R2 to accumulate an intermediate similar to $\mathbf{H}_{peroxo}$, the putative peroxodiiron(III) complex from the methane monooxygenase catalytic cycle. J. Am. Chem. Soc 1998;120:1094–1095.
35. Skulan AJ, Brunold TC, Baldwin J, Saleh L, Bollinger JM Jr, Solomon EI. Nature of the peroxo intermediate of the W48F/D84E ribonucleotide reductase variant: implications for O_2 activation by binuclear non-heme iron enzymes. J. Am. Chem. Soc 2004;126:8842–8855. [PubMed: 15250738]
36. Yun D, Garcìa-Serres R, Chicalese BM, An YH, Huynh BH, Bollinger JM Jr. (μ-1,2-Peroxo)diiron (III/III) complex as a precursor to the diiron(III/IV) intermediate **X** in the assembly of the iron-radical cofactor of ribonucleotide reductase from mouse. Biochemistry 2007;46:1925–1932. [PubMed: 17256972]
37. Saleh L, Krebs C, Ley BA, Naik S, Huynh BH, Bollinger JM Jr. Use of a chemical trigger for electron transfer to characterize a precursor to cluster **X** in assembly of the iron-radical cofactor of *Escherichia coli* ribonucleotide reductase. Biochemistry 2004;43:5953–5964. [PubMed: 15147179]
38. Bennati M, Weber A, Antonic JLD, Perlstein, Robblee J, Stubbe J. Pulsed ELDOR spectroscopy measures the distance between the two tyrosyl radicals in the R2 subunit of the *E.coli* ribonucleotide reductase. J. Am. Chem. Soc 2003;125:14988–14989. [PubMed: 14653724]
39. Bennati M, Robblee JH, Mugnaini V, Stubbe J, Freed JH, Borbat P. EPR distance measurements support a model for long-range radical initiation in *E. coli* ribonucleotide reductase. J. Am. Chem. Soc 2005;127:15014–15015. [PubMed: 16248626]
40. Climent I, Sjöberg B-M, Huang CY. Site-directed mutagenesis and deletion of the carboxyl terminus of *Escherichia coli* ribonucleotide reductase protein R2. Effects on catalytic activity and subunit interaction. Biochemistry 1992;31:4801–4807. [PubMed: 1591241]

41. Ekberg M, Sahlin M, Eriksson M, Sjöberg B-M. Two conserved tyrosine residues in protein R1 participate in an intermolecular electron transfer in ribonucleotide reductase. J. Biol. Chem 1996;271:20655–20659. [PubMed: 8702814]
42. Rova U, Goodtzova K, Ingemarson R, Behravan G, Gräslund A, Thelander L. Evidence by site-directed mutagenesis supports long-range electron transfer in mouse ribonucleotide reductase. Biochemistry 1995;34:4267–4275. [PubMed: 7703240]
43. Rova U, Adrait A, Pötsch S, Gräslund A, Thelander L. Evidence by mutagenesis that Tyr^{370} of the mouse ribonucleotide reductase R2 protein is the connecting link in the intersubunit radical transfer pathway. J. Biol. Chem 1999;274:23746–23751. [PubMed: 10446134]
44. Saleh L, Bollinger JM Jr. Cation mediation of radical transfer between Trp48 and Tyr356 during O_2 activation by protein R2 of *Escherichia coli* ribonucleotide reductase: relevance to R1–R2 radical transfer in nucleotide reduction? Biochemistry 2006;45:8823–8830. [PubMed: 16846225]
45. Seyedsayamdost MR, Yee CS, Reece SY, Nocera DG, Stubbe J. pH rate profiles of F_nY_{356}-R2s (n = 2, 3, 4) in *Escherichia coli* ribonucleotide reductase: Evidence that Y_{356} is a redox-active amino acid along the radical propagation pathway. J. Am. Chem. Soc 2006;128:1562–1568. [PubMed: 16448127]
46. Seyedsayamdost MR, Stubbe J. Site-specific replacement of Y356 with 3,4-dihydroxyphenylalanine in the β2 subunit of *E. coli* ribonucleotide reductase. J. Am. Chem. Soc 2006;128:2522–2523. [PubMed: 16492021]
47. Seyedsayamdost MR, Stubbe J. Forward and reverse electron transfer with the Y_{356}DOPA-β2 heterodimer of *E. coli* ribonucleotide reductase. J. Am. Chem. Soc 2007;129:2226–2227. [PubMed: 17279757]
48. Seyedsayamdost MR, Xie J, Chan CTY, Schultz PG, Stubbe J. Site-specific insertion of 3-aminotyrosine into subunit α2 of *E. coli* ribonucleotide reductase: direct evidence for involvement of Y_{730} and Y_{731} in radical propagation. J. Am. Chem. Soc 2007;129:15060–15071. [PubMed: 17990884]
49. Voevodskaya N, Narvaez AJ, Domkin V, Torrents E, Thelander L, Gräslund A. Chlamydial ribonucleotide reductase: tyrosyl radical function in catalysis replaced by the Fe^{III}-Fe^{IV} cluster. Proc. Natl. Acad. Sci. U.S.A 2006;103:9850–9854. [PubMed: 16777966]
50. Jiang W, Bollinger JM Jr, Krebs C. The active form of *Chlamydia trachomatis* ribonucleotide reductase R2 protein contains a heterodinuclear Mn(IV)/Fe(III) cluster with $S = 1$ ground state. J. Am. Chem. Soc 2007;129:7504–7505. [PubMed: 17530854]
51. Atkin CL, Thelander L, Reichard P, Lang G. Iron and free radical in ribonucleotide reductase. Exchange of iron and Mössbauer spectroscopy of the protein B2 subunit of the *Escherichia coli* enzyme. J. Biol. Chem 1973;248:7464–7472. [PubMed: 4355582]
52. Bossek U, Weyhermüller T, Wieghardt K, Bonvoisin J, Girerd JJ. Synthesis, E.S.R. spectrum and magnetic properties of a heterobinuclear complex containing the $\{Fe^{III}(\mu\text{-}O)(\mu\text{-}MeCO_2)_2Mn^{III}\}^{2+}$ core. J. Chem. Soc., Chem. Commun 1989;10:633–636.
53. Thelander L, Larsson B, Hobbs J, Eckstein F. Active site of ribonucleoside diphosphate reductase from *Escherichia coli*. Inactivation of the enzyme by 2'-substituted ribonucleoside diphosphates. J. Biol. Chem 1976;251:1398–1405. [PubMed: 767333]
54. Sjöberg B-M, Gräslund A, Eckstein F. A substrate radical intermediate in the reaction between ribonucleotide reductase from *Escherichia coli* and 2'-azido-2'-deoxyribonucleoside diphosphates. J. Biol. Chem 1983;258:8060–8067. [PubMed: 6305969]
55. Fritscher J, Artin E, Wnuk S, Bar G, Robblee JH, Kacprzak S, Kaupp M, Griffin RG, Bennati M, Stubbe J. Structure of the nitrogen-centered radical formed during inactivation of *E. coli* ribonucleotide reductase by 2'-azido-2'-deoxyuridine-5'-diphosphate: Trapping of the 3'-ketonucleotide. J. Am. Chem. Soc 2005;127:7729–7738. [PubMed: 15913363]
56. Voevodskaya N, Lendzian F, Ehrenberg A, Gräslund A. High catalytic activity achieved with a mixed manganese-iron site in protein R2 of Chlamydia ribonucleotide reductase. FEBS Lett 2007;581:3351–3355. [PubMed: 17601579]
57. Bollinger JM Jr, Jiang W, Green MT, Krebs C. The manganese(IV)/iron(III) cofactor of *Chlamydia trachomatis* ribonucleotide reductase: Structure, assembly, radical initiation, and evolution. Curr. Opin. Struct. Biol. accepted

58. Jiang W, Hoffart LM, Krebs C, Bollinger JM Jr. A manganese(IV)/iron(IV) intermediate in assembly of the manganese(IV)/iron(III) cofactor of *Chlamydia trachomatis* ribonucleotide reductase. Biochemistry 2007;46:8709–8716. [PubMed: 17616152]
59. Zheng M, Khangulov SV, Dismukes GC, Barynin VV. Electronic structure of dimanganese(II,III) and dimanganese(III,IV) complexes and dimanganese catalase enzyme: a general EPR spectral simulation approach. Inorg. Chem 1994;33:382–387.
60. Lee S-K, Fox BG, Froland WA, Lipscomb JD, Münck E. A transient intermediate of the methane monooxygenase catalytic cycle containing an $Fe^{IV}Fe^{IV}$ cluster. J. Am. Chem. Soc 1993;115:6450–6451.
61. Lee SK, Nesheim JC, Lipscomb JD. Transient intermediates of the methane monooxygenase catalytic cycle. J. Biol. Chem 1993;268:21569–21577. [PubMed: 8408008]
62. Shu L, Nesheim JC, Kauffmann KE, Münck E, Lipscomb JD, Que L Jr. An $Fe_2^{IV}O_2$ diamond core structure for the key intermediate **Q** of methane monooxygenase. Science 1997;275:515–518. [PubMed: 8999792]
63. Nordlund P, Sjöberg B-M, Eklund H. Three-dimensional structure of the free radical protein of ribonucleotide reductase. Nature 1990;345:593–598. [PubMed: 2190093]
64. Eriksson M, Jordan A, Eklund H. Structure of *Salmonella typhimurium* nrdF ribonucleotide reductase in its oxidized and reduced forms. Biochemistry 1998;37:13359–13369. [PubMed: 9748343]
65. Jiang W, Saleh L, Barr EW, Xie J, Maslak Gardner M, Krebs C, Bollinger JM Jr. Branched activation- and catalysis-specific pathways for electron relay to the manganese/iron cofactor in ribonucleotide reductase from *Chlamydia trachomatis*. Biochemistry 2008;47:8477–8484. [PubMed: 18656954]
66. Jiang W, Xie J, Nørgaard H, Bollinger JM Jr, Krebs C. Rapid and quantitative activation of *Chlamydia trachomatis* ribonucleotide reductase by hydrogen peroxide. Biochemistry 2008;47:4477–4483. [PubMed: 18358006]
67. Sahlin M, Sjöberg B-M, Backes G, Loehr T, Sanders-Loehr J. Activation of the iron-containing B2 protein of ribonucleotide reductase by hydrogen peroxide. Biochem. Biophys. Res. Comm 1990;167:813–818. [PubMed: 2182022]
68. Willing A, Follmann H, Auling G. Ribonucleotide reductase of *Brevibacterium ammoniagenes* is a manganese enzyme. Eur. J. Biochem 1988;170:603–611. [PubMed: 2828045]
69. Huque Y, Fieschi F, Torrents E, Gibert I, Eliasson R, Reichard P, Sahlin M, Sjöberg B-M. The active form of the R2F protein of class Ib ribonucleotide reductase from *Corynebacterium ammoniagenes* is a diferric protein. J. Biol. Chem 2000;275:25365–25371. [PubMed: 10801858]

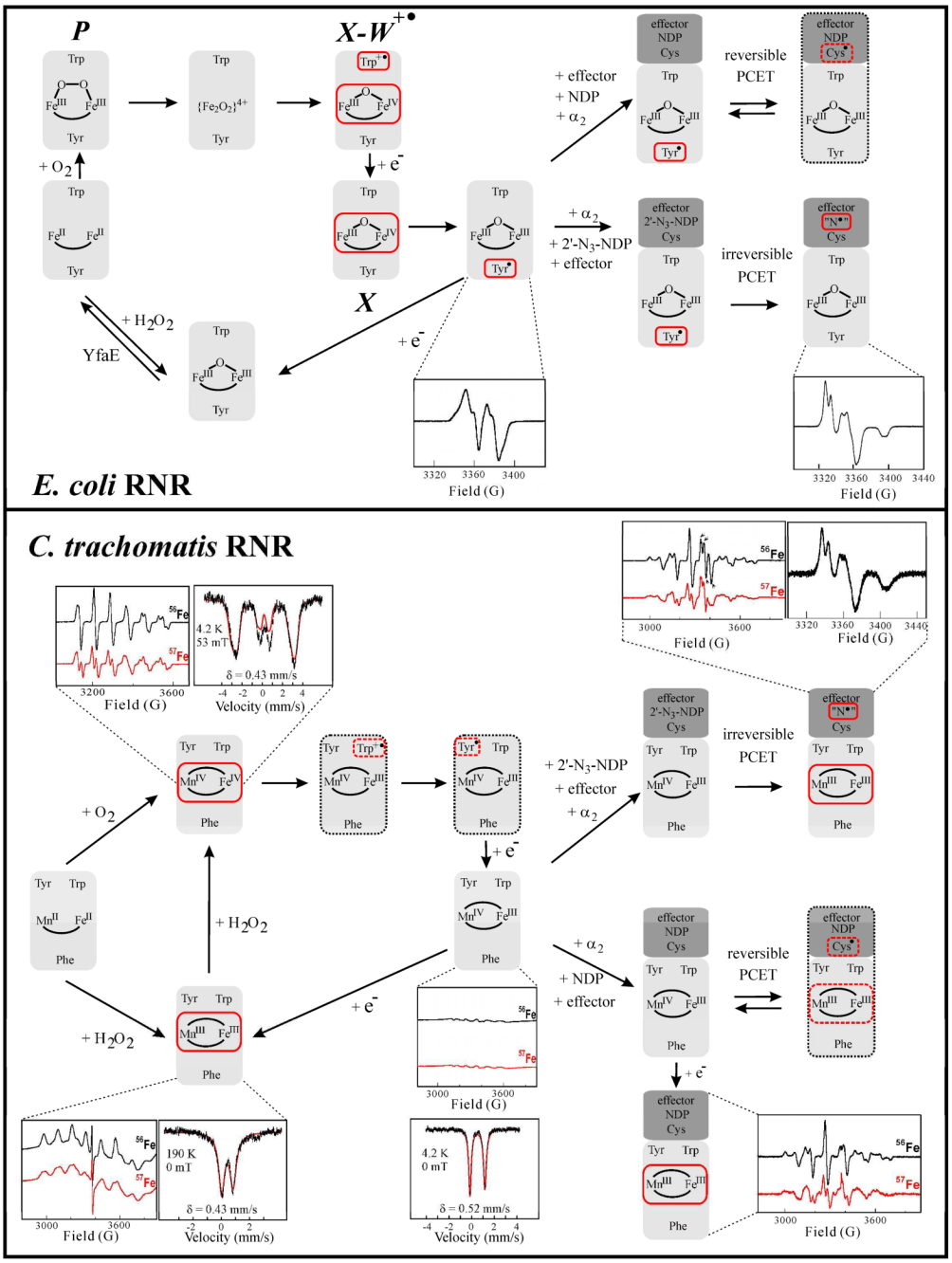

Figure 1.

Assembly, maintenance, and role in catalysis of the $Fe_2^{III/III}$-Y• and Mn^{IV}/Fe^{III} cofactors of *Ec* β_2 (top) and *Ct* β_2 (bottom). The red boxes indicate EPR active states. States encircled with a grey dotted line have not been directly detected. Selected EPR and Mössbauer spectra of various states are also shown. The 3'-H-cleaving C• in α_2 has not been detected in either enzyme. However, copious indirect evidence, including structural analogy to the class II enzyme (12) in which the C• *was* directly detected (7), indicates that it forms in the *Ec* enzyme and by analogy the *Ct* enzyme. The spectrum of the N• in *Ec* RNR was adapted from (4).

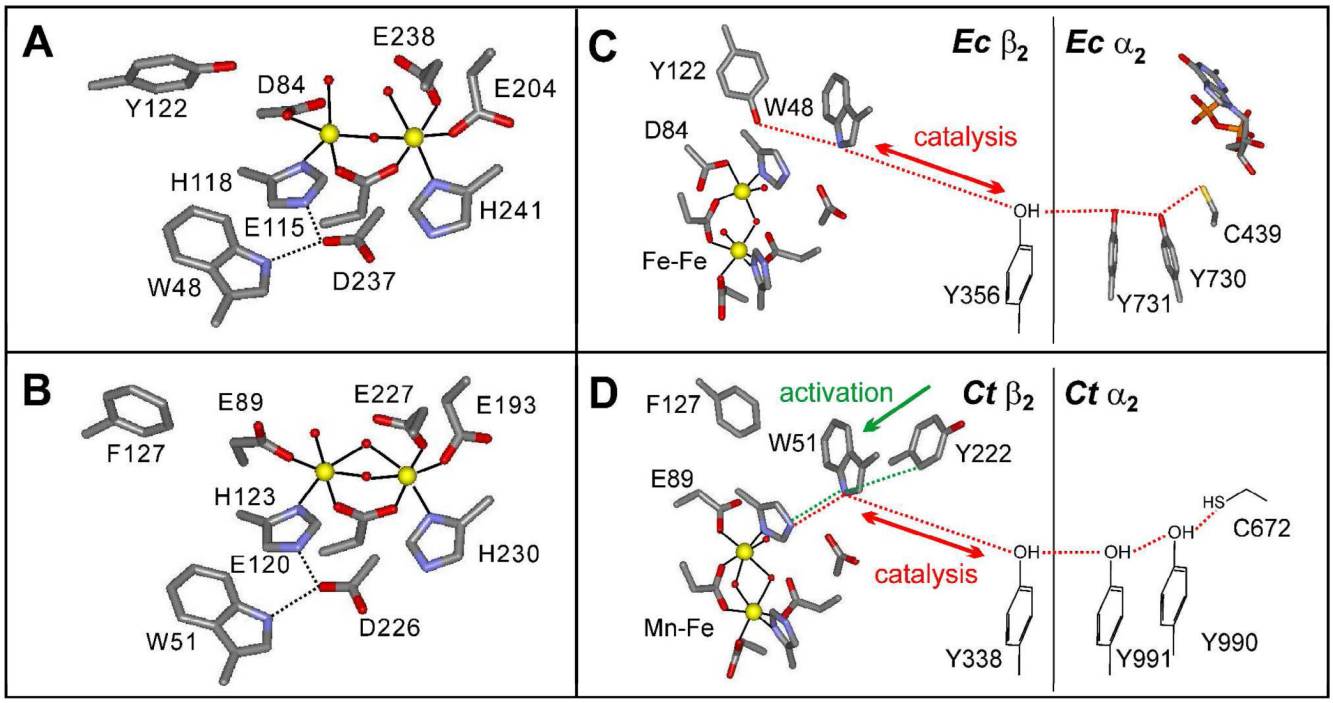

Figure 2.

Structural models of the $Fe_2^{III/III}$ clusters in (**A**) *Ec* and (**B**) *Ct* β_2s (pdb codes 1MXR and 1SYY, respectively). Schematic representations of the proposed PCET pathways in (**C**) *Ec* and (**D**) *Ct* RNR. (**C**) and (**D**) are adapted from (12) and (65), respectively.

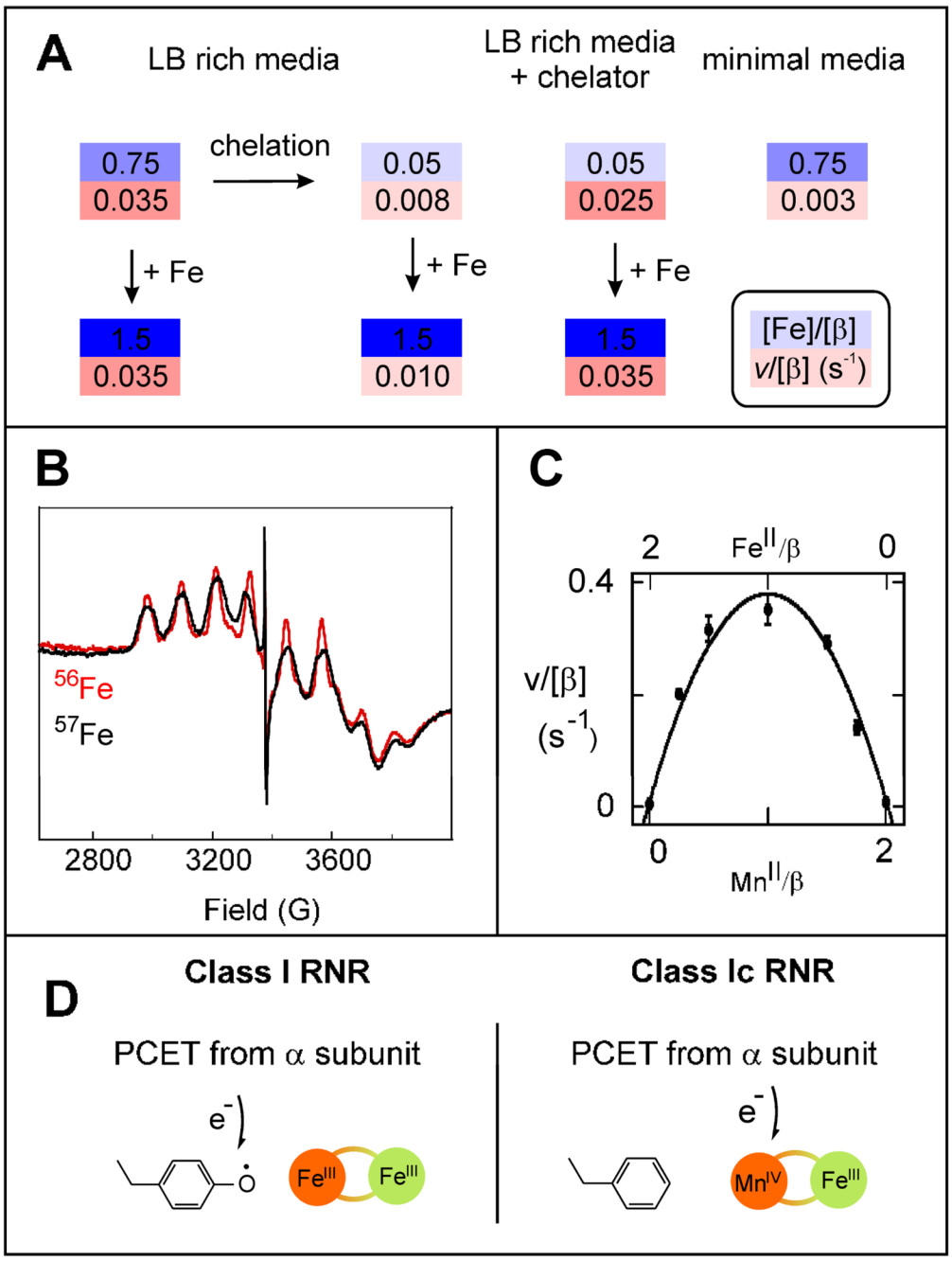

Figure 3.

(**A**) Comparison of Fe/β (top, on blue shaded part) and activity/β (s^{-1}) (bottom, on red shaded part) for *Ct* β_2 prepared and treated in different ways. (**B**) EPR spectra of *Ct* β_2 that was isolated from *Ec* cells grown on rich medium, depleted of its Fe, reconstituted with 1.5 Fe^{II}/β (either natural abundance or >95% enriched ^{57}Fe), dialyzed to remove excess Fe, and reduced with 20 mM dithionite for 2 min at 22 °C. Spectrometer conditions: T = 4 K, ν = 9.45 GHz, power = 20 mW, modeulation amplitude = 10 G modulation amplitude, scan time = 167 s, and time constant = 167 ms. (**C**) Dependence of the catalytic activity of *Ct* β on the equivalencies of Mn^{II} and Fe^{II} at a constant total metal equivalency of 2/β; adapted from (17). (**D**) Schematic

representation of the radical-generating cofactors of class Ia/b (top) and class Ic (bottom) RNRs; adapted from (50).